NUKLEONIKA 2007;52(3):87–91

ORIGINAL PAPER

Studies on a low energy plasma focus discharge

Tarek M. Allam,
Samar Tawfik Abd El-Latif,
Hanaa M. Soliman

Abstract. This paper is devoted to the experimental and theoretical study of plasma current sheath behavior for a low energy plasma focus device operating at a filling nitrogen gas pressure of 3.3 torr, and at a stored energy of 1.2 kJ. Axial distribution profiles of plasma current sheath (PCS) characteristics such as propagation velocity V_z, acceleration a_z, azimuthal magnetic field induction B_θ, and magnetic force per unit volume F_z/m^3 along the coaxial electrodes system was performed from a magnetic probe and miniature Rogovsky coil signals. The experimental results showed that the axial distribution of V_z, a_z, B_θ and F_z has approximately the same profile and the maximum value of these parameters was detected nearly at a mid-distance of coaxial electrodes system. Theoretical description of PCS dynamics at the axial phase, based on a snowplough, was estimated as a function of discharge time. These data were compared with the received experimental results.

Key words: plasma focus • plasma sheath dynamics • magnetic force • focusing action

T. M. Allam, S. Tawfik Abd El-Latif✉, H. M. Soliman
Plasma Physics and Nuclear Fusion Department,
Nuclear Research Center,
Atomic Energy Authority,
Inshas, Abo-Zabal, P. O. Box 13759, Cairo, Egypt,
Tel.: +202 4620807, Fax: +202 22876031,
E-mail: samar_tawfik2004@yahoo.com

Received: 5 February 2007
Accepted: 4 July 2007

Introduction

Since the advent of plasma focus discharge some years ago, investigators have made different studies to determine the PCS dynamics during the axial acceleration phase of discharge. Some of these studies have been reported by many laboratories [1–4]. Silva P *et al*. [4] studied the characterization of a very small plasma focus in the low energy (50 J) and at a hydrogen filling pressure of 470 mbar. These authors observed that at the end of coaxial electrodes the PCS has a shape like an umbrella and the pinch after the radial is clear. They indicated that these results are similar to the results obtained with device operating at energies several orders of magnitude higher. El-Kashef GM, Soliman HM [1] studied the distribution of magnetic forces in axial, radial and azimuthal direction for a 4.4 kJ plasma focus device and their dependence on helium gas pressure in the range from 0.5 to 1.5 torr. They found that the maximum forces along the interelectrode space are reported at a pressure of 1 torr. Measurements of magnetic profiles in a 3.6 kJ plasma focus device operated in air with a pressure in the range from 0.5 to 1 torr was performed by Mathuthu M *et al*. [2]. These authors showed that the current sheath carries only 68.5% of total current. A rapid drop of the magnetic field at a mid-distance of coaxial electrodes suggested that

a mass and diffuse current shedding occur after a mid-distance in the focus tube. Investigation of cumulative flows in a 4 kJ plasma focus with different gas filling a plasma focus chamber was performed by Nikulin VYa *et al*. [3]. They found that the velocity of axial flow depends on the sort of gas and is about 3×10^7 cm/s for deuterium and 2×10^7 cm/s for argon. The shape of the flow is changed from a broad conical fly for deuterium to quasi one-directional stream in the case of argon.

This paper presents a study of the effects of nitrogen gas pressure on the focusing time of plasma discharge and the PCS dynamics during the acceleration phase for a low energy plasma focus discharge.

Experimental setup

The nitrogen gas is admitted to the annular space between two coaxial electrodes through four orifices drilled at equal distances on a circular path around the surface of the inner electrode, each one is 0.6 cm in diameter. Also, there are six small glass windows fixed on the surface of the outer electrode for optical observations. Each window is of 1 cm diameter.

This device is powered by a capacitor bank with a maximum stored energy of 4.2 kJ, and it is switched by an ignitron tube and a high current triggering pulse.

Figure 1a shows a schematic diagram of the essential parts of the plasma focus device. Figure 1b shows a scheme of the plasma focus chamber and location of magnetic probe technique. The coaxial plasma focus device is consisted of two stainless-steel coaxial electrodes. The inner and outer major and minor diameters of cylindrical electrodes are 2.58 cm, 2 cm and 8.9 cm, 8.25 cm respectively, with lengths of 20 cm and 60 cm correspondingly. The inner and outer electrodes are separated at the coaxial electrodes breech by a prespex insulator in the shape of a cylinder of length 4 cm, major diameter of 8.2 cm and minor diameter of 2.62 cm.

Results and discussion

Measurements of focus time, peak discharge current time and axial transit time (t_a) of PCS at axial distance z = 1.5 cm from breech at different filling nitrogen gas pressures in the range from 0.5 to 4 torr with 1.2 kJ stored in the capacitor bank are performed by a Rogovsky coil and magnetic probe techniques.
Figure 2a shows the electrical signals for the total current and the current derivative for shots in nitrogen gas at p = 3.3 torr. Figure 2b shows that the minimum difference between the focusing time which is indicated

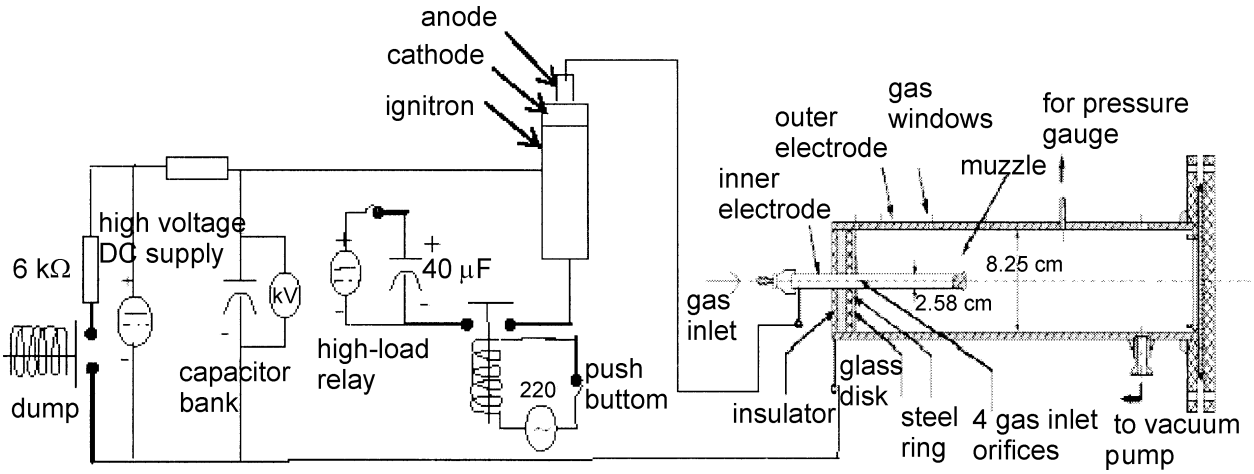

Fig. 1a. A schematic layout of the plasma focus device.

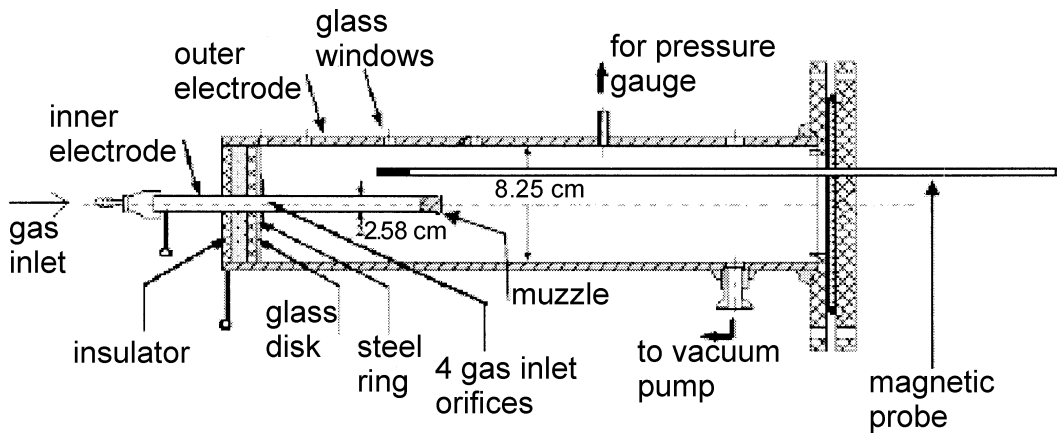

Fig. 1b. A schematic diagram of plasma focus chamber.

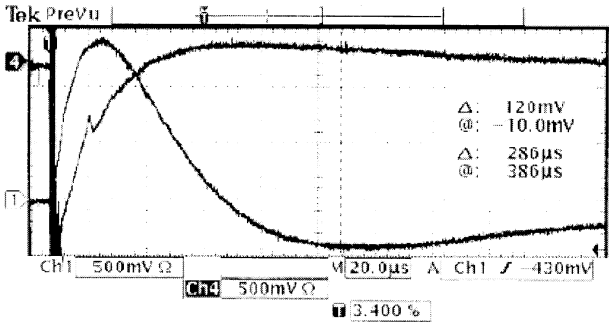

Fig. 2a. Electrical signals of total current and current derivative at p = 3.3 torr, a typical dip (plasma focus) in the signal of the current derivative is observed.

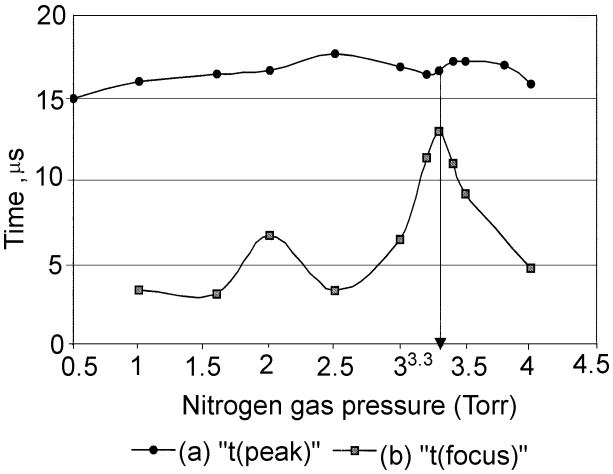

Fig. 2b. The time-to-peak of discharge current vs. nitrogen gas pressure (a) and focus time vs. nitrogen gas pressure (b).

by the current dip and the peak discharge current time at p = 3.3 torr. Also this figure clears that under a gas pressure of 1 torr and above 4 torr no focus is observed, at such pressures a non-homogeneous initial PCS is formed.

Figure 3 demonstrates that, the minimum value of t_a was detected at approximately p = 3.3 torr. From the above results, it is clear that the gas pressure = 3.3 torr is most suitable for the experimental work on this device.

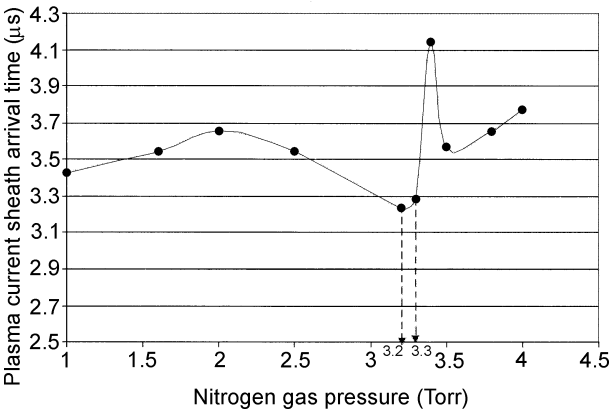

Fig. 3. Nitrogen gas pressure vs. plasma current sheath arrival time.

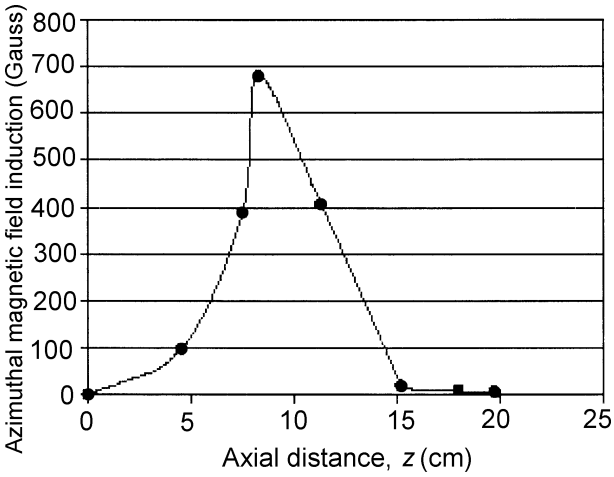

Fig. 4. The magnetic field induction vs. axial distance z of the discharge chamber.

Plasma current sheath dynamics along the coaxial electrodes, z and at a mid-distance of the annular space between two coaxial electrodes system are done by two successive magnetic probes and a miniature Rogovsky coil technique.

Figure 4 presents the variation of azimuthal magnetic field induction B_θ, against the axial distance z. As can be seen B_θ presents a maximum value of 696.667 G at z = 9 cm, and decreases with increasing z. The axial PCS velocity V_z and acceleration a_z along the coaxial electrodes are estimated from the arrival time of PCS from the start of discharge time until it reached a coaxial electrodes muzzle data (Figs. 5a, 5b, 5c).

These figures reveal that V_z and a_z have a maximum value of 1.25×10^7 cm/s and 24.71×10^{12} cm/s^2 at $z \sim 11.3$ cm and at $z \sim 7.2$ cm, respectively and after this a sharp dumping is observed, which is mainly due to adiabatic expansion phenomena.

The axial magnetic force per unit volume F_z/m^3 which causes the plasma mass to be accelerated axially along the coaxial electrodes system, is evaluated from the simultaneous measurements of the radial current density through the plasma and azimuthal magnetic field induction. Variation of F_z/m^3 with axial distance z is shown in Fig. 6 which illustrates that F_z/m^3 has approximately the same behavior like B_θ and has a maximum value of 7.29×10^2 N/m^3 at $z \approx 8$ cm.

Theoretical analysis of PCS dynamics during the axial phase is evaluated by a snowplough model [6], in which all the gas is swept by the PCS propagates within the interelectrode space of the coaxial system.

By using the Navier Stokes equation and snowplough model then the axial PCS position z (under the same experimental discharge conditions) can be calculated from the relation

$$z^2 = \frac{\mu_0 \ln\left(\frac{b'}{a}\right)}{\rho\pi^2\left(b'^2 - a^2\right)} \iint I^2 dt^2 \quad (1)$$

where: $b' = (a + b)/2 = 2.7075$ cm; I is the discharge current; ρ (the ambient gas density) and $\rho = 4.887 \times 10^{-3}$ kg/m^3.

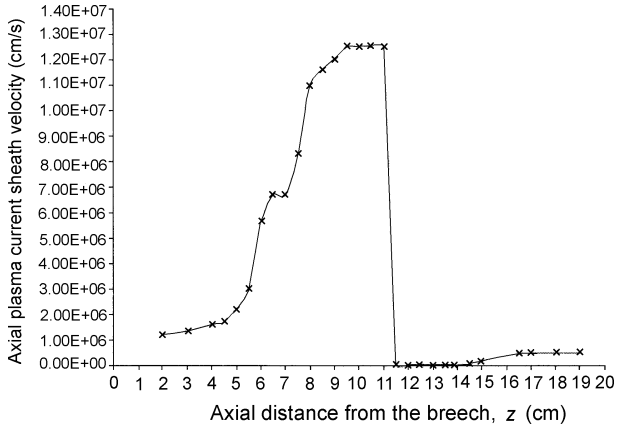

Fig. 5a. The variation of axial plasma sheath velocity with respect to the z distance from the breech to coaxial electrodes muzzle.

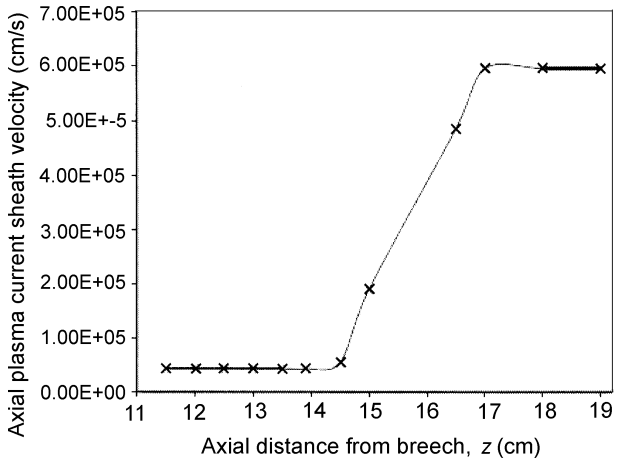

Fig. 5b. The plasma sheath velocity vs. axial z distance from z = 11.5 to coaxial electrodes muzzle.

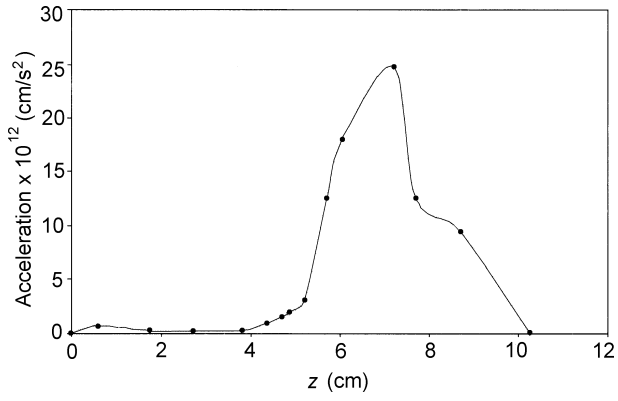

Fig. 5c. The variation of axial plasma sheath acceleration with respect to the z distance from the breech.

From the data of variation of discharge current with discharge time t and with the aid of origin program, then it has a sine damping function equation as

$$I = Ae^{\frac{-t}{t_0}} \sin\left(\pi \frac{(t - x_c)}{\lambda}\right) \tag{2}$$

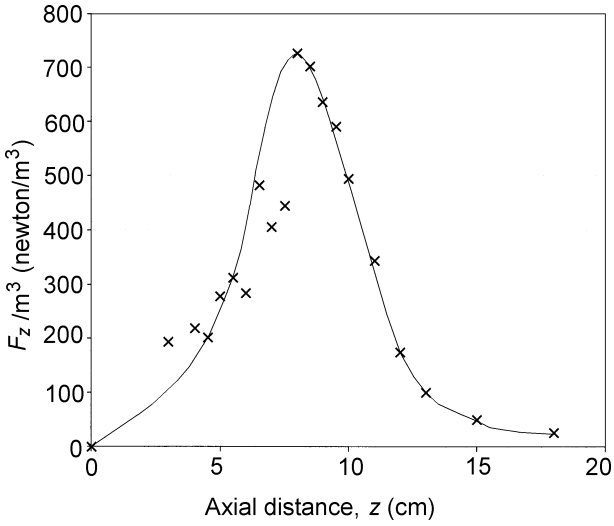

Fig. 6. The variation of the magnetic force density F_z/m^3 vs. z distance from the breech.

where: A (which represent the amplitude) = 3805.82309 and error ± 152.5006; t_0 (which represent the decay constant) = 0.00003 and error ± 1.3666×10^{-6}; x_c (which represent the center) = 0 and error ± 3.0783×10^{-7}; λ (which represent the width) = 0.00005 and error ± 7.9244×10^{-7}.

Then, for simplicity the equation of the discharge current is in the form of

$$I = Ae^{\frac{-t}{t_0}} \sin\left(\pi \cdot \frac{t}{\lambda}\right) \tag{3}$$

where t is the time of discharge current I.

On substituting Eq. (3) in Eq. (1) the axial distance z has then the form:

$$z = k\left\{k'\left\{\begin{array}{l}\dfrac{t_0^2}{4}e^{\frac{-2t}{t_0}}\sin^2\left(\dfrac{\pi t}{\lambda}\right)+\dfrac{t_0^3\pi}{4\lambda}e^{\frac{-2t}{t_0}}\sin\left(\dfrac{2\pi t}{\lambda}\right)\\ +\dfrac{t_0^4\pi^2}{8\lambda^2}e^{\frac{-2t}{t_0}}-\dfrac{t_0^4\pi^2}{4\lambda^2}+\dfrac{t_0^4\pi^2}{8\lambda^2}e^{\frac{-2t}{t_0}}\cos\left(\dfrac{2\pi t}{\lambda}\right)\end{array}\right\}\right.$$
$$\left.+\frac{t_0^4\pi^2}{8\lambda^2}e^{\frac{-2t}{t_0}}-\frac{t_0^4\pi^2}{8\lambda^2}+\frac{t_0^3\pi^2}{4\lambda^2}t\right\}^{\frac{1}{2}} \tag{4}$$

where k and k' are constants = 354.04 and 0.2, respectively.

Figure 7 shows the relation between the theoretical calculations and the experimental measurements of axial distance traveled by the PCS from the beginning of discharge time until t = 4.8 μs and z = 11.3 cm (condition of maximum measured axial velocity).

This figure illustrates that the distance z increases with increasing discharge time. From these figures, the ratio of $(\rho_{theoretical}/\rho_{experimental})\%$ can be estimated as

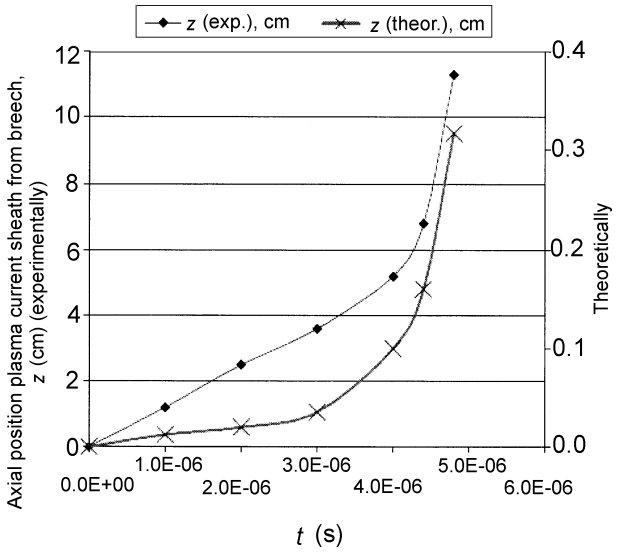

Fig. 7. Time variation of axial plasma current sheath position from the breech (experimentally, and theoretically).

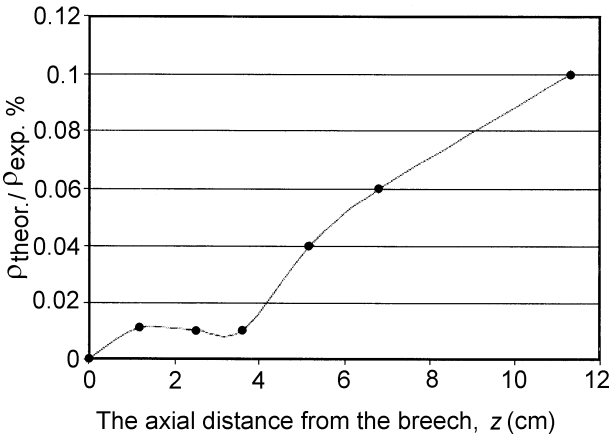

Fig. 8. The relation of $(\rho_{theoretical}/\rho_{experimental})\%$ against the axial distance from the breech.

shown in Fig. 8. This figure demonstrates that the mention above ratio has a maximum value ≈ 0.1% at $z = 11.3$ cm, i.e. at the position of $(V_z)_{max}$.

Conclusion

Experimental results of focus action, i.e. the effect of nitrogen gas pressure on focusing time, concluded that the focusing action is a very sensitive function of gas pressure and the optimum operating pressure is detected at $p = 3.3$ torr.

Results of axial distribution of PCS velocity V_z, acceleration a_z, magnetic force per unit volume F_z/m^3 and azimuthal magnetic field induction B_θ behind a PCS along the coaxial electrodes and at radial distance ≈ 2.7075 cm from inner electrode surface demonstrated that they have the same behavior and the maximum value of the these parameters is detected approximately at a mid-distance of interelectrode discharge region. After this a damping of V_z and a_z is observed which was due to 3-d adiabatic expansion of PCS [5].

Finally, the behavior of PCS dynamics along the coaxial electrodes may be originated from the fact that the PCS was more canted at an approximately middle distance of coaxial electrodes and the PCS rim near the inner electrode was reached the coaxial electrodes muzzle. After this distance expanded of PCS was detected.

The numerical calculations based on a snowplough model yielded that the time distribution of PCS position along the coaxial electrodes is lower than that measured experimentally. The discrepancy between the calculated and the measured value could be attributed due to the fact that experimentally the PCS does not carry along with it all the gas particles encountered, then the motion mass, i.e. gas density ρ of the snowplough model is greater than the actual one.

References

1. El-Kashef GM, Soliman HM (2003) Magnetic forces distribution in 4.4 kJ plasma focus device. In: Proc of the 1st Cairo Conf on Plasma Physics and Application CCPPA 2003, Cairo, Egypt 34:166–169
2. Mathuthu M, Zengeni TG, Gholap AR (1996) Measurement of magnetic field and velocity profiles in 3.6 kJ. United Nations University/International Center for Theoretical Physics Plasma Focus Fusion Device. Phys Plasma 3:4572–4576
3. Nikulin VYa, Krokhin ON, Gurei AE, Polukhin SN, Tikhomiror AA (2001) Investigation of cumulative flows in plasma focus. In: Proc of the Int Symp Research and Application of Plasmas, Warsaw, Poland 1:72–76
4. Silva P, Soto L, Moreno J *et al.* (2001) Characterization of a very small plasma focus in the limit of low energy. In: Proc of the Int Symp Research and Application of Plasmas, Warsaw, Poland 563:235–239
5. Soliman HM, El-Kashef GM, Masoud MM (1994) Coaxial discharge and transverse magnetic field. Plasma Phys 34:587–591
6. Tsagas NF, Mair GLR, Prinn AE (1978) Motion and shape of snowplough sheets in coaxial accelerators. Phys D 11:1263–1272